

# Statistical description and dimension reduction of categorical trajectories with multivariate functional principal components

Hervé CARDOT<sup>1</sup> and Caroline PELTIER<sup>2,3</sup>

<sup>1</sup>Institut de Mathématiques de Bourgogne, UMR CNRS 5584, Université Bourgogne Europe, Dijon, France

<sup>2</sup>Inrae, Centre des Sciences du Goût et de l’Alimentation, UMR CNRS-INRAE-Institut Agro, Dijon, France

<sup>3</sup>Probe Research Infrastructure, Chemosens facility, CNRS-INRAE, Dijon, France

September 9, 2025

## Abstract

There are many examples in which the statistical units of interest are samples of a continuous time categorical random process, that is to say a continuous time stochastic process taking values in a finite state space. Getting simple representations that allow comparisons of a set of trajectories is of major interest for statisticians. Without loosing any information, we associate to each state a binary random function, taking values in  $\{0, 1\}$ , and turn the problem of statistical description of the categorical trajectories into a multivariate functional principal components analysis. The (multivariate) covariance operator has nice interpretations in terms of departure from independence of the joint probabilities and the multivariate functional principal components are simple to interpret. Under the weak hypothesis assuming only continuity in probability of the  $0 - 1$  trajectories, it is simple to build consistent estimators of the covariance kernel and perform multivariate functional principal components analysis. The sample paths being piecewise constant, with a finite number of jumps, this a rare case in functional data analysis in which the trajectories are not supposed to be continuous and can be observed exhaustively. The approach is illustrated on a data set of sensory perceptions, considering different gustometer-controlled stimuli experiments. We also show how it can be easily extended to analyze experiments, such as temporal check-all-that-apply, in which two states or more can be observed at the same time.

**Keywords** : categorical functional data, continuous time categorical processes, dimension reduction, discontinuous trajectories, sensometrics, temporal dominance of sensations, temporal check all that apply

## 1 Introduction

A lot of attention has been paid in the statistical literature over the last decades to develop tools dedicated to the analysis and modeling of functional data, considering random trajectories

defined on an interval  $[0, T]$  and taking values in  $\mathbb{R}$ , at each  $t \in [0, T]$  (see for example Gertheiss et al. (2024) and Koner and Staicu (2023) for recent reviews of the literature and Ramsay and Silverman (2005) for a seminal reference on functional data analysis). Much less attention has been given to the case in which the trajectories take values in a finite set of elements that are not necessarily numbers, that is to say when  $\mathbb{R}$  is replaced by the finite set  $\mathcal{S} = \{S_1, \dots, S_q\}$ , with cardinality  $q$ .

However, there are many examples in which the statistical units of interest are samples of a continuous time random categorical process : in a pioneer work on demographic studies, Deville (1982) extended the notion of multiple correspondence analysis to continuous time correspondence analysis in order to analyze the time evolution of the "marital status" of a sample of women over the period [1962, 1975]. The trajectories related to the marital status take values in a state space  $\mathcal{S}$  with  $q = 4$  states (divorced, married, single, widowed). Recent examples of statistical analysis of individual categorical trajectories are found in food science, a domain in which it is of great interest to get information about the temporal perception of aliments to understand the perception mechanisms. Of particular interest is the Temporal Dominance of Sensations (TDS) approach which consists in choosing sequentially attributes, among a list composed of  $q$  predefined items, describing a food product over tasting (see Pineau et al. (2009)). The chosen states correspond to the most striking perception at a given time and the results of TDS experiments, after time normalization, can be represented via barplots as in Figure 1. The technique developed by Deville (1982), also called qualitative harmonic analysis (see Deville and Saporta (1980)) or categorical functional data analysis (CFDA) is now available in **R**, package **cfda** (see Preda et al. (2021)) and can be used to analyze such kind of data. Even if the CFDA approach can be very powerful by encoding categorical trajectories into a sequence of real components (see Peltier et al. (2023) for an illustration in sensory analysis), the interpretation of the results in terms of individual trajectories is often delicate.

Statistical approaches based on Markov processes and their extensions (see Lindsey (2012) for an overview and Limnios and Oprişan (2001) for an introduction to semi-Markov processes) can be useful to fit the law of the trajectories at the population level and to provide a simple representation of the dynamics via the graph of transitions between states. Considering parametric distributions for the sojourn time in the different states also allows to deal with maximum likelihood estimation techniques, permitting to build two-sample tests to compare two populations (*e.g* two food products or two categories of consumers (see Cardot and Frascolla (2024)) as well as model-based clustering, considering mixtures of semi-Markov processes (see Cardot et al. (2019)). A major drawback of this approach is that it is not well suited for analyzing data at the individual level, and the Markovian assumption is often too simplistic to properly fit real data. Additionally, it is difficult to apply when more than one state can be present simultaneously (see the TCATA experiment described in Section 4.2), as this requires

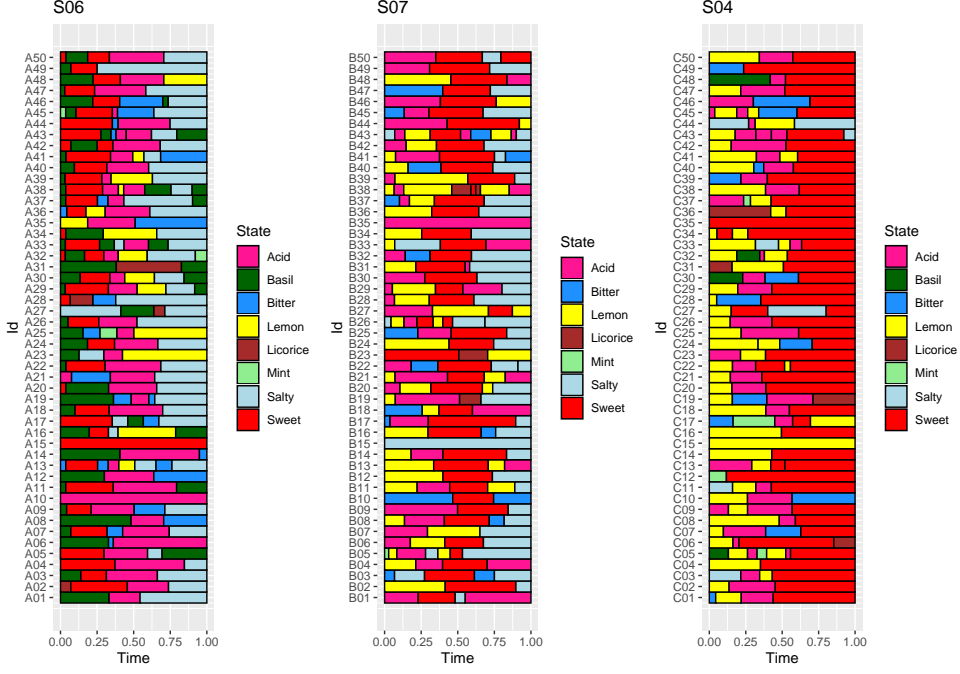


Figure 1: TDS bandplot for  $n = 150$  tasting experiments and  $q = 8$  states, considering three different gustometer-controlled stimuli, S06, S07 and S04, extracted from the open data basis Béno et al. (2023). Each row corresponds to a categorical trajectory.

drastically increasing the number of system states to  $2^q$  to account for all possible combinations.

In this work, we introduce another point of view and associate to each state  $S_j$ , for  $j = 1, \dots, q$ , a random trajectory  $X_j(t), t \in [0, T]$ , taking value 1 when state  $S_j$  is observed at time  $t$  and zero else. The information given by a categorical trajectory  $Y$  is equivalent to the information given by the  $q$  binary 0-1 trajectories  $X_1, \dots, X_q$ .

One could consider such trajectories as compositional data evolving over time (see Aitchison (1983) for a seminal paper and Greenacre (2021) for a recent review on compositional data analysis). A major difficulty to deal with compositional data approaches in our framework is due to the fact that we deal with individual trajectories so that, at each instant  $t$ ,  $q - 1$  individual observations, among  $X_1(t), \dots, X_q(t)$ , have value 0. In other words, at each instant  $t$ , all the observed units are on the vertices of the simplex, so that usual logarithmic transforms cannot apply directly.

Our approach is based on the optimal approximation, according to the  $L^2$  distance, to such 0-1 trajectories in a small dimension functional space. This leads us to consider the multivariate functional principal component analysis (MFPCA, see Chiou et al. (2014) or Happ and Greven (2018)) of the multivariate functional vector  $\mathbf{X} = (X_1, \dots, X_q)$ . We show that it leads both to principal components that can be simply interpreted in terms of variations around the mean probability curve related to each state, and powerful tools able to reduce effectively the dimension of categorical functional data in a finite dimension vector space. All codes in the

R language are available on Github, <https://github.com/Chemosens/ExternalCode/tree/main/MFPCAwithCategoricalTrajectories>.

## 2 Notations and mathematical framework

To describe continuous time categorical trajectories, as those drawn in Figure 1, we consider the random element  $Y = \{Y(t), t \in [0, T]\}$ , with  $Y(t) \in \mathcal{S} = \{S_1, \dots, S_q\}$  for all  $t \in [0, T]$ . We denote by  $p_j(t) = \mathbb{P}[Y(t) = S_j]$ , the probability of being in state  $S_j$  at time  $t$  and, for  $(s, t) \in [0, T] \times [0, T]$  and  $(j, \ell) \in \{1, \dots, q\} \times \{1, \dots, q\}$ , the joint probability

$$p_{j\ell}(s, t) = \mathbb{P}[Y(s) = S_j \text{ and } Y(t) = S_\ell].$$

We associate to  $Y$ ,  $q$  trajectories  $X_j$ ,  $j = 1, \dots, q$ , related to the occurrence of state  $S_j$ , and defined as follows,  $X_j(t) = 1$  if  $Y(t) = S_j$  and 0 otherwise. In other words,  $X_j(t) = \mathbf{1}_{\{Y(t)=S_j\}}$ , for all  $t \in [0, T]$ , where  $\mathbf{1}_{\{\cdot\}}$  is the indicator function. We clearly have

$$\begin{aligned} \mathbb{E}[X_j(t)] &= \mathbb{E}[\mathbf{1}_{\{Y(t)=S_j\}}] \\ &= p_j(t) \end{aligned}$$

and

$$\begin{aligned} \mathbb{E}[X_j(s)X_\ell(t)] &= \mathbb{E}[\mathbf{1}_{\{Y(s)=S_j\}}\mathbf{1}_{\{Y(t)=S_\ell\}}] \\ &= p_{j\ell}(s, t). \end{aligned}$$

We suppose in the following that hypothesis **H**<sub>1</sub> is satisfied

$$\mathbf{H}_1 : \lim_{h \rightarrow 0} \mathbb{P}[Y(t) \neq Y(t+h)] = 0, \quad \forall t \in [0, T]$$

ensuring that the trajectories  $X_j$ ,  $j = 1, \dots, q$  are continuous in probability. Hypothesis **H**<sub>1</sub> prevents them to have too many jumps or to have jumps that occur at the same time point  $t_0$  with non null probability. Define the covariance functions  $\gamma_j(s, t) = \text{Cov}(X_j(s), X_j(t))$  and, for  $\ell \neq j$ ,  $\gamma_{j\ell}(s, t) = \text{Cov}(X_j(s), X_\ell(t))$ . We remark that  $\gamma_j(t, t) = p_j(t)(1 - p_j(t))$  and  $\gamma_{j\ell}(s, t) = p_{j\ell}(s, t) - p_j(s)p_\ell(t)$ , so that the terms out of the diagonal, when  $s \neq t$ , can be related to a departure from independence.

**Proposition 2.1.** *Under hypothesis **H**<sub>1</sub>, we have for all  $j \in \{1, \dots, q\}$ ,*

- $p_j$  (resp.  $\gamma_j$ ) is continuous on  $[0, T]$  (resp. on  $[0, T] \times [0, T]$ )
- $\gamma_{j\ell}$  is continuous on  $[0, T] \times [0, T]$ , for all  $\ell \neq j$ .

*Proof.* of Proposition 2.1

Remarking that  $\sup_{t \in [0, T]} |X_j(t)| \leq 1$  almost surely, we deduce, by Theorem 1.3.6 in Serfling (1980), that the trajectories are also continuous in the  $L^2$  sense (or mean square continuous) when  $\mathbf{H}_1$  is true, that is to say

$$\lim_{h \rightarrow 0} \mathbb{E} \left[ (X_j(t) - X_j(t+h))^2 \right] = 0, \quad \forall t \in [0, T], \quad \forall j \in \{1, \dots, q\}. \quad (1)$$

The continuity  $p_j$  and  $\gamma_{jj}$  is a consequence of Theorem 7.3.2 in Hsing and Eubank (2015) which states that the mean  $p_j$  and covariance functions  $\gamma_{jj}$  are continuous if and only if  $X_j$  is mean-square continuous. To prove the continuity of  $\gamma_{j\ell}$ , we note that for  $(s, t)$  and  $(s', t')$  in  $[0, T] \times [0, T]$ , we get thanks to the Cauchy-Schwarz inequality,

$$\begin{aligned} |\gamma_{j\ell}(s, t) - \gamma_{j\ell}(s', t')| &\leq |\mathbb{Cov}(X_j(s) - X_j(s'), X_\ell(t))| + |\mathbb{Cov}(X_j(s'), X_\ell(t) - X_\ell(t'))| \\ &\leq \sqrt{\gamma_{\ell\ell}(t) \mathbb{E} \left[ (X_j(s) - X_j(s'))^2 \right]} + \sqrt{\gamma_{jj}(s) \mathbb{E} \left[ (X_\ell(t) - X_\ell(t'))^2 \right]} \end{aligned}$$

and we conclude using (1).  $\square$

Note that the binary trajectories  $X_j$  take values in the Hilbert space  $L^2[0, T]$  equipped with the usual inner product, denoted by  $\langle \cdot, \cdot \rangle$ , and norm  $\|\cdot\|$ . Denote by  $\Gamma_{j\ell} : L^2[0, T] \rightarrow L^2[0, T]$  the cross-covariance operator between  $X_j$  and  $X_\ell$ . It is the integral operator with kernel function  $\gamma_{j\ell}(s, t)$ ,

$$\Gamma_{j\ell} f(s) = \int_0^T (p_{j\ell}(s, t) - p_j(s)p_\ell(t)) f(t) dt. \quad (2)$$

Considering now simultaneously  $X_1, \dots, X_q$ , we denote by  $\mathbf{X} = (X_1, \dots, X_q)$  the random vector of functions, that takes values in  $\mathbb{H} = L^2[0, T] \times \dots \times L^2[0, T]$ , the Hilbert space of  $q$  dimensional vectors of functions in  $L^2[0, T]$ , equipped with the inner product

$$\langle \mathbf{f}, \mathbf{g} \rangle_{\mathbb{H}} = \sum_{j=1}^q w_j \langle f_j, g_j \rangle. \quad (3)$$

The weights  $w_j$  that can be chosen by the statistician (see Remark 2 below and Section 4) are strictly positive. We denote by  $\mathbf{p} = (p_1, \dots, p_q) \in \mathbb{H}$  the expectation of  $\mathbf{X}$ ,  $\mathbf{p} = \mathbb{E}[\mathbf{X}]$ , and by  $\mathbf{\Gamma} : \mathbb{H} \rightarrow \mathbb{H}$  the covariance operator. It satisfies,  $\forall \boldsymbol{\phi} = (\phi_1, \dots, \phi_q) \in \mathbb{H}$ ,

$$\mathbf{\Gamma} \boldsymbol{\phi}(s) = \mathbb{E} [\langle \mathbf{X} - \mathbf{p}, \boldsymbol{\phi} \rangle_{\mathbb{H}} (\mathbf{X}(s) - \mathbf{p}(s))], \quad (4)$$

$$= \sum_{\ell=1}^q w_\ell \begin{pmatrix} \Gamma_{1\ell} \phi_\ell(s) \\ \vdots \\ \Gamma_{q\ell} \phi_\ell(s) \end{pmatrix} \quad (5)$$

We denote by  $\boldsymbol{\gamma}(s, t)$  the corresponding (weighted) multivariate covariance function, with elements  $(w_\ell \gamma_{j\ell}(s, t))_{j,\ell}$ . We deduce from Proposition 2.1 and the multivariate version of Mercer's theorem (see Chiou et al. (2014) or Happ and Greven (2018)) that there exists a set of

orthonormal basis functions  $\phi_r(s) = (\phi_{r1}(s), \dots, \phi_{rq}(s))$  in  $\mathbb{H}$ ,  $r = 1, 2, \dots$  and corresponding eigenvalues  $\lambda_1 \geq \lambda_2 \geq \dots \geq 0$  such that

$$\gamma(s, t) = \sum_{r \geq 1} \lambda_r \phi_r(s) \phi_r(t)^\top.$$

This leads to the following expansion of the covariance functions  $\gamma_{j\ell}(s, t)$ ,

$$p_{j\ell}(s, t) - p_j(s)p_\ell(t) = \sum_{r \geq 1} \lambda_r \phi_{rj}(s) \phi_{r\ell}(t). \quad (6)$$

It is not difficult to show that operator  $\mathbf{\Gamma}$ , defined in (4), is the integral operator with kernel function  $\gamma(s, t)$  and  $\mathbf{\Gamma}\phi_r = \lambda_r \phi_r$ . Furthermore,  $\sum_{r \geq 1} \lambda_r = \mathbb{E} [\|\mathbf{X} - \mathbf{p}\|_{\mathbb{H}}^2] \leq T \max_j w_j$ .

The optimal linear expansion of  $\mathbf{X} - \mathbf{p}$  in a  $k$  dimensional vector space of  $\mathbb{H}$ , in terms of quadratic mean, is given by the truncated Karhunen-Loëve expansion  $\tilde{\mathbf{X}}_k$  of  $\mathbf{X}$ ,

$$\tilde{\mathbf{X}}_k(t) = \mathbf{p} + \sum_{r=1}^k \langle \mathbf{X} - \mathbf{p}, \phi_r \rangle_{\mathbb{H}} \phi_r(t). \quad (7)$$

Our aim is to estimate  $\mathbf{p}$  and  $\phi_r$ , for  $r = 1, \dots, k$ , in order to be able to capture the main variations of a categorical random function  $Y$  in a small  $k$  dimensional vector space.

**Remark 1.** *The continuous time extension of correspondence analysis, named qualitative harmonic analysis and developed by Deville (1982) and Deville and Saporta (1980) is based on the eigen decomposition of another integral operator, with a purpose that is not to expand the trajectories themselves in an "optimal" way but to relate the states  $S_j$  to numerical values at each instant  $t$ . More precisely, the aim is to find an optimal encoding function  $\varphi : \mathcal{S} \times [0, 1] \rightarrow \mathbb{R}$  minimizing the following criterion*

$$\int_0^T \int_0^T \mathbb{E} [(\varphi(Y(t), t) - \varphi(Y(s), s))^2] ds dt$$

*subject to identifiability constraints  $\mathbb{E} [\varphi(Y_t, t)] = 0$  for all  $t \in [0, 1]$  and unit variance,  $\int_0^T \mathbb{E} [\varphi(Y(t), t)^2] dt = 1$ . A solution  $\varphi(x, t)$  satisfies, for all  $x \in \mathcal{S}$ , the integral operator equation (see equation (42) in Deville (1982)),*

$$\sum_{\ell=1}^q \int_0^T \frac{p_{j\ell}(t, s)}{p_j(t)p_\ell(s)} \varphi(S_\ell, s) p_\ell(s) ds = \lambda \varphi(x, t), \quad \forall t \in [0, T]. \quad (8)$$

*Departure from independence is evaluated via the ratio  $\frac{p_{j\ell}(t, s)}{p_j(t)p_\ell(s)}$  which is equal to one in case of independence. Denoting by  $\tilde{\lambda}_1 \geq \tilde{\lambda}_2 \geq \dots \geq 0$  the sequence eigenvalues of operator equation (8) and by  $\varphi_i(t) = (\varphi_i(S_1, t), \dots, \varphi_i(S_q, t))$  the eigenfunction related to  $\tilde{\lambda}_i$ , we get a Mercer type expansion of the joint probabilities (see equation (43) in Deville (1982)),*

$$p_{j\ell}(t, s) = p_j(t)p_\ell(s) \left( \sum_{r \geq 1} \tilde{\lambda}_i \varphi_i(S_j, t) \varphi_i(S_\ell, s) \right). \quad (9)$$

This means that the optimal encoding approach considers implicitly a multiplicative point of view to expand the departure from independence of the joint probabilities  $p_{j\ell}(s, t)$  whereas the optimal trajectory expansion studied in this article considers an additive point of view, as seen in (6).

**Remark 2.** If the statistician wants to give the same importance to all the states, one reasonable option consists in choosing weights

$$\begin{aligned} w_j &= \frac{1}{\text{tr}(\Gamma_{jj})} \\ &= \left( \int_0^T p_j(t) (1 - p_j(t)) dt \right)^{-1} \end{aligned} \quad (10)$$

setting to one the trace of the covariance operator  $(w_j)^{-1}\Gamma_{jj}$  of the binary (normalized) trajectory  $X_j$ .

**Remark 3.** Previous framework can be extended easily to experiments in which more than two states can be present simultaneously without increasing the cardinality of  $\mathcal{S}$  (see the TCATA experiment described in Section 4.2). If we replace  $\mathbf{H}_1$  by the hypothesis that the trajectories  $X_1, \dots, X_q$  are continuous in probability, Proposition 2.1 remains true.

### 3 Sampling and estimators

Suppose now we have a sample of  $n$  categorical trajectories  $Y_1, \dots, Y_n$  observed over  $[0, T]$  and taking values in  $\mathcal{S} = \{S_1, \dots, S_q\}$ . We define  $\mathbf{X}_i = (X_{i1}, \dots, X_{iq})$  the vector of the  $q$  corresponding binary trajectories, with  $X_{ij}(t) = \mathbf{1}_{\{Y_i(t) = S_j\}}$ . These trajectories are piecewise constant, with a finite number of jumps. It is a rare case in functional data analysis in which the trajectories can be observed exhaustively, that is to say for all time point  $t \in [0, T]$ .

We consider, for all  $s$  and  $t$  in  $[0, T]$ , the empirical probabilities of occurrence  $\hat{p}_j(t) = n^{-1} \sum_{i=1}^n X_{ij}(t)$  and  $\hat{\mathbf{p}}(t) = (\hat{p}_1(t), \dots, \hat{p}_q(t))$ . We also consider the joint empirical probabilities  $\hat{p}_{j\ell}(s, t) = n^{-1} \sum_{i=1}^n X_{ij}(s) X_{i\ell}(t)$ , and define the estimators of the covariance functions

$$\hat{\gamma}_j(t, t) = \hat{p}_j(t)(1 - \hat{p}_j(t))$$

and

$$\hat{\gamma}_{j\ell}(s, t) = \hat{p}_{j\ell}(s, t) - \hat{p}_j(s)\hat{p}_\ell(t).$$

We deduce from (2), estimators  $\hat{\Gamma}_{j\ell}$  of the cross-covariance operators  $\Gamma_{j\ell}$  and from (5), an estimator  $\hat{\Gamma}$  of  $\Gamma$ . Note that in a more formal way, we can express

$$\begin{aligned} \hat{\mathbf{p}} &= \frac{1}{n} \sum_{i=1}^n \mathbf{X}_i \\ \hat{\Gamma} &= \sum_{i=1}^n \mathbf{X}_i \otimes \mathbf{X}_i - \hat{\mathbf{p}} \otimes \hat{\mathbf{p}} \end{aligned}$$

where the tensor product is defined as follows,  $(\mathbf{u} \otimes \mathbf{v}) \phi = \langle \mathbf{u}, \phi \rangle_{\mathbb{H}} \mathbf{v}$  for all  $\mathbf{u}, \mathbf{v}, \phi$  belonging to  $\mathbb{H}$ . We can state the following consistency and asymptotic normality results which follow immediately from assumption **H**<sub>1</sub>. We denote by  $\|\Gamma\|_{op}$  the spectral norm of linear operator  $\Gamma$  induced by the norm in  $\mathbb{H}$ .

**Proposition 3.1.** *Suppose that hypothesis **H**<sub>1</sub> is fulfilled, as  $n$  tends to infinity,*

- $\|\widehat{\mathbf{p}} - \mathbf{p}\|_{\mathbb{H}} \rightarrow 0$  and  $\|\widehat{\Gamma} - \Gamma\|_{op} \rightarrow 0$  almost surely,
- $\sqrt{n}(\widehat{\mathbf{p}} - \mathbf{p})$  and  $\sqrt{n}(\widehat{\Gamma} - \Gamma)$  are asymptotically Gaussian.

*Proof.* of Proposition 3.1

First note that  $\mathbb{H}$  equipped with the inner product  $\langle \cdot, \cdot \rangle_{\mathbb{H}}$  is a separable Hilbert space. We clearly have

$$\begin{aligned} \|\mathbf{X}\|_{\mathbb{H}}^2 &= \sum_{j=1}^q w_j \|X_j\|^2 \\ &\leq T \max_j w_j, \end{aligned}$$

so that all the moments of  $\|\mathbf{X}\|_{\mathbb{H}}$  are finite. The proposition is then a direct consequence of Theorems 8.1.1 and 8.1.2 in Hsing and Eubank (2015) that are stated in general separable Hilbert spaces, considering the empirical mean  $\widehat{\mathbf{p}} = \frac{1}{n} \sum_{i=1}^n \mathbf{X}_i$  and the empirical covariance operator  $\widehat{\Gamma} = \frac{1}{n} \sum_{i=1}^n \mathbf{X}_i \otimes \mathbf{X}_i - \widehat{\mathbf{p}} \otimes \widehat{\mathbf{p}}$ .  $\square$

We can deduce from Proposition 3.1 the consistency and asymptotic normality of the estimators of the eigenvalues  $\widehat{\lambda}_r$ ,  $r = 1, \dots, k$  (see Dauxois et al. (1982) or Theorem 9.1.3 in Hsing and Eubank (2015)). Under the additional assumption that the eigenvalues are distinct, we can also get the asymptotic normality of the estimated eigenfunctions  $\widehat{\phi}_r(t)$ ,  $r = 1, \dots, k$ .

## 4 Two illustrations in sensory analysis

The dataset used for illustration deals with sensory experiments. It is well documented in Béno et al. (2023) and can be obtained from a public source. In each illustration fifty panelists took part in a tasting experiment and were asked to click on the sensation they perceived in real time from a list of descriptors. Computations were performed with the library MFPCA (see Happ (2022)) in the **R** language R Core Team (2024). All codes are available on Github, <https://github.com/Chemosens/ExternalCode/tree/main/MFPCAWithCategoricalTrajectories>.

When participants are instructed to click only on the dominant sensation, i.e. when only one perception can be observed at any given time, the protocol is called Temporal Dominance of Sensation" (TDS, see Pineau et al. (2009) for a reference article). When participants are

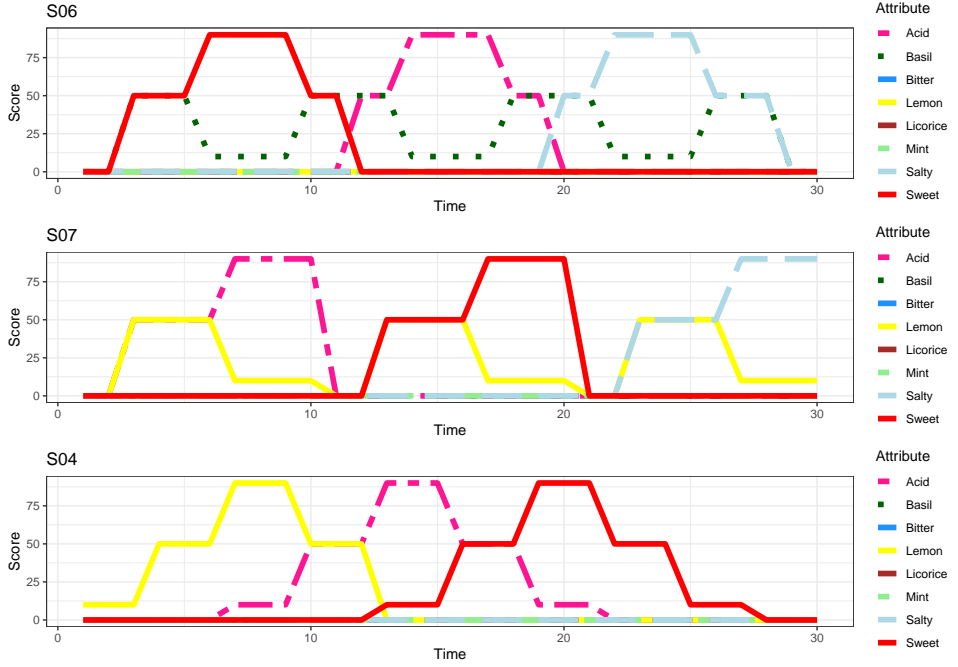


Figure 2: Three gustometer-controlled stimuli (S06, S07 and S04) extracted from the open data basis Béno et al. (2023).

asked to click on all the sensations they perceive in real time from the same list of descriptors, the protocol is called Temporal Check-All-That-Apply (TCATA, see Castura et al. (2016) for a seminal article). Unlike the TDS protocol, several descriptors (or none at all) can be selected at any given time for TCATA experiments. The resulting data consists of binary trajectories linked to each state, with the value 0 when a descriptor is unclicked at time  $t$  and 1 when it is clicked. Thus the difference between TCATA and TDS data is that at each instant  $t$ , the sum of all binary trajectories can be different from 1 and take values in the set  $\{0, 1, \dots, q\}$  for TCATA whereas the sum is always equal to 1 for TDS.

In all the experiments, the tasted temporal solution is controlled and delivered by a gustometer. Three controlled sensory signals (see Figure 2) were tasted by the panelists: S04 (Lemon, followed by Acid, and finally Sweet), S06 (Sweet, Acid, and finally Salty, with a continuous hint of Basil), and S07 (Acid, followed by Sweet, and finally Salty, with a continuous hint of Lemon). The descriptor list included Acid, Sweet, Lemon, Basil, and Salty, alongside distractors such as Mint, Licorice and Bitter, so that the categorical process  $Y$  has  $q = 8$  states.

The overall number of experiments is  $n = 150$  and time has been normalized to be  $[0, 1]$  for each experiment, resulting, for TDS, in the observed categorical trajectories drawn in Figure 1.

#### 4.1 Temporal dominance of sensation (TDS) trajectories

Most statistical analyses for TDS data are, until now, based on the examination of the evolution over time of the proportion  $\hat{p}_j(t)$  of occurrence of each state  $j$  (see Pineau et al. (2009)), as

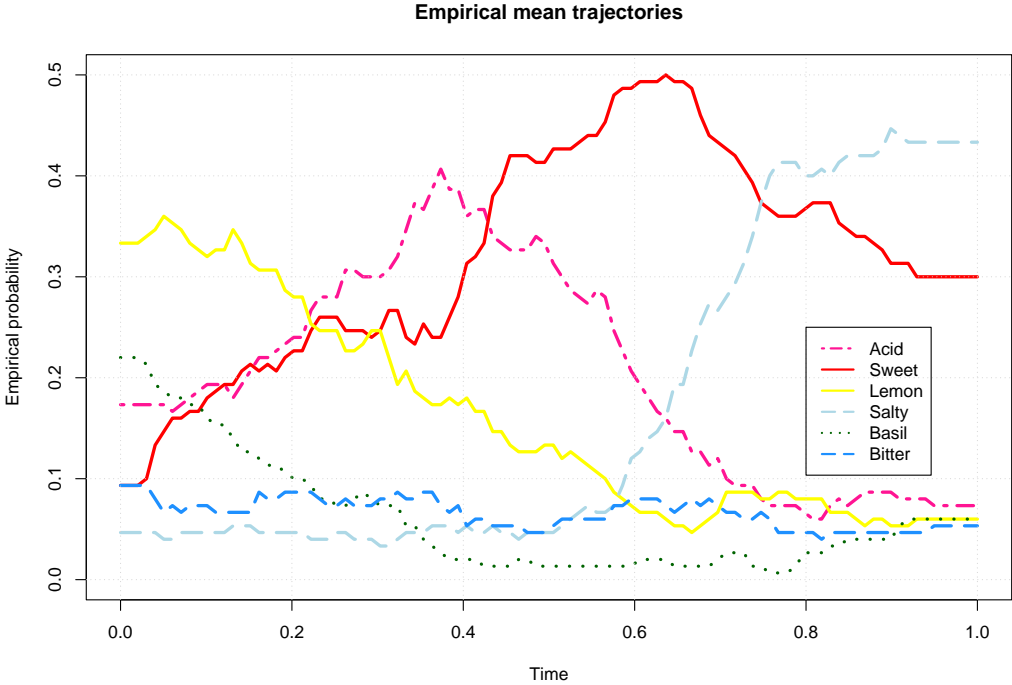


Figure 3: Empirical probabilities  $\hat{p}_j(t)$ ,  $t \in [0, 1]$ . The curves are drawn only for the states  $j$  whose average probability of occurrence is larger than 5%, that is to say  $\int_0^1 \hat{p}_j(t) dt \geq 0.05$

shown in Figure 3. The interpretation is then generally based on the succession of the most frequently observed states, and would lead to say, in that experiment, that the first dominant sensation is Lemon, followed by Acid, Sweet and to finish by Salty. As seen below, the signal is much more complex since we are, in this controlled experiment, in presence of three different subpopulations (S04, S06 and S07), which are not detected with the average approach that does not take account of individual temporal variations.

A multivariate FPCA of the trajectories  $\mathbf{X}_i$ ,  $i = 1, \dots, n$ , considering equal weights  $w_j = 1/q$  for  $j = 1, \dots, q$  has been performed, giving the same weight to all states  $S_1, \dots, S_q$  (see the Appendix for the the analysis considering weights given in (10)). The first eigenvalue  $\lambda_1$  represents 23% of the total variance, whereas the second one  $\lambda_2$  represents 11% of the total variance, the third one 7% and the fourth one 6%. The decrease of the eigenvalues to zero is rather slow (see Figure 4), which is not so surprising since the  $\mathbf{X}_i$  trajectories are not continuous.

The estimated principal component scores  $\langle \mathbf{X}_i - \hat{\mathbf{p}}, \hat{\phi}_r \rangle_{\mathbb{H}}$ , for  $r = 1, 2$  are drawn in Figure 5, whereas the main variations around the mean functions, for the first two dimensions, are drawn in Figure 6 and Figure 7. For better interpretation and graphical representation, we only consider the components  $j$  with the largest variations, that is to say with the largest values of  $\|\hat{\phi}_{rj}\|$ ,  $j = 1, \dots, q$ . Since, for each value of  $r$ ,  $\|\hat{\phi}_r\|_{\mathbb{H}}^2 = 1$ , we can build the following indicator

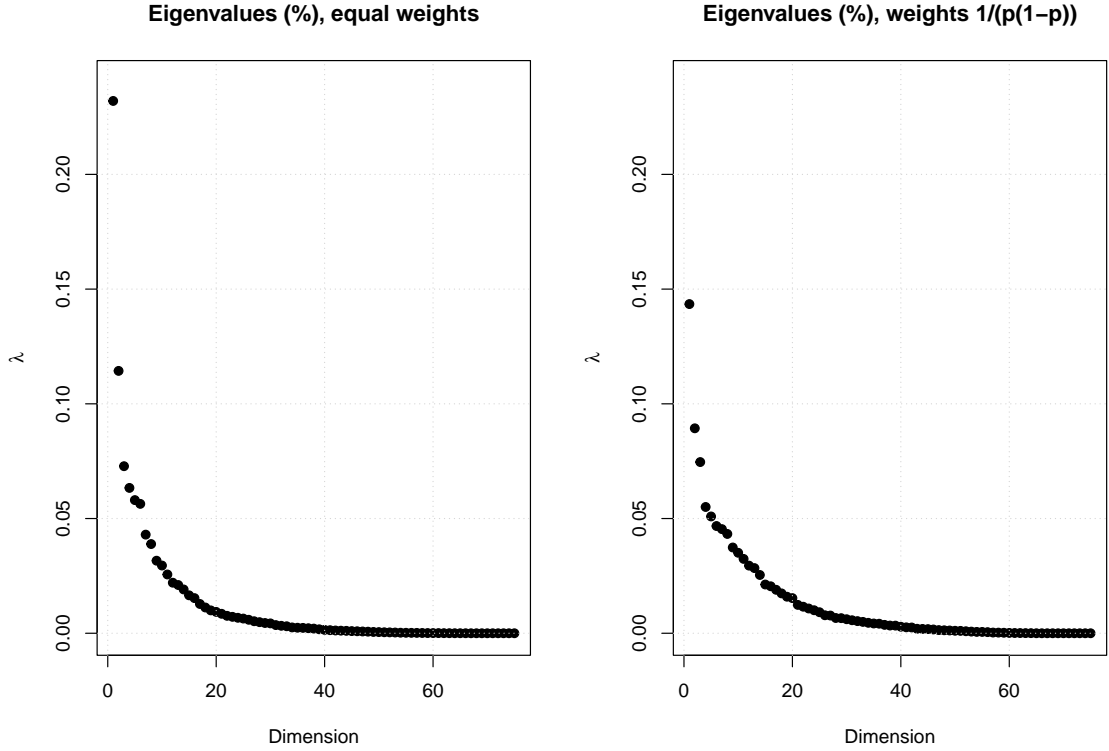


Figure 4: Proportion of total variance captured by the principal components considering equal weights  $w_1 = \dots = w_q$  on the left and weights as in (10) on the right.

of importance of each category  $j$  in dimension  $r$ ,

$$\text{imp}_{rj} = w_j \|\hat{\phi}_{rj}\|^2, \quad (11)$$

with  $\sum_{j=1}^q \text{imp}_{rj} = 1$ , and consider only the most important variables (see Table 1). This leads us to select for graphical representation of the eigenfunctions the states Acid, Lemon, Salty and Sweet for the first dimension and Acid, Basil, Salty and Sweet for the second dimension.

The results are simple to interpret. For example, the black dots in Figure 5, corresponding to the S04 experiment, are characterized by a first principal component taking positive values, related, as seen in Figure 6, to a high probability of occurrence of Lemon and small probability of occurrence of Sweet at the beginning of the period, and a high probability of occurrence of Sweet and a small probability of occurrence of Salty at the end of the period. These results on Lemon and Sweet are in agreement with the original signal S04, that was first Lemon, then Acid and finally Sweet (see Figure 2). It was the only controlled signal to be not salty at the end of the tasting. Regarding the Acid attribute, it is also present in S06 (middle of tasting) and S07 (beginning of tasting) and this is why it is not highlighted in the first principal components.

This is the opposite situation for the S06 experiment whose observations (in grey dots) are related to a negative value of the first principal component. The light grey dots, that correspond to the S07 experiment are characterized by negative values of the second principal

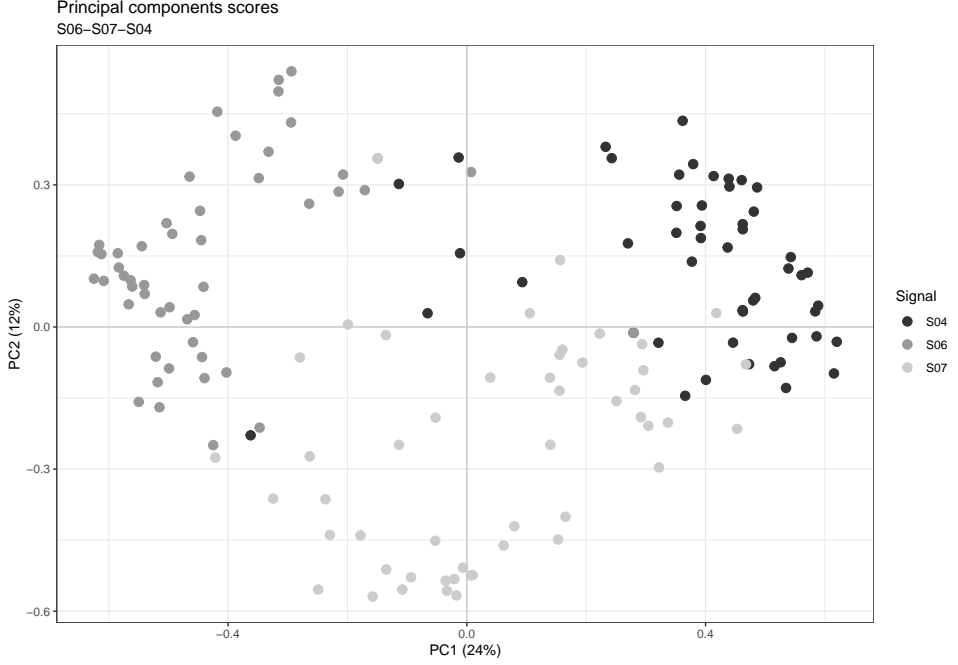


Figure 5: Estimated principal component scores with equal weights  $w_j$ . Different colours are used to distinguish the observations according to the set of customer-controlled stimuli.

	dim 1	dim 2	dim 3
Acid	0.08	0.26	0.42
Basil	0.04	0.07	0.00
Bitter	0.00	0.02	0.01
Lemon	0.10	0.02	0.48
Licorice	0.00	0.00	0.00
Mint	0.00	0.00	0.00
Salty	0.22	0.30	0.02
Sweet	0.56	0.34	0.06

Table 1: Importance of the different states on each dimension of the MFPCA with equal weights  $w_j$ .

components. A look at Figure 7 indicates that negative values on the second axis correspond to high probability to be Acid at the beginning of the tasting, Sweet in the middle and Salty at the end. These are exactly the main features of the S07 signal (see Figure 2).

## 4.2 Temporal Check All That Apply experiments (TCATA)

In the same dataset Béno et al. (2023), the same gustometer signals (S04, S06, and S07) were also evaluated using the Temporal Check-All-That-Apply protocol but with another panel of

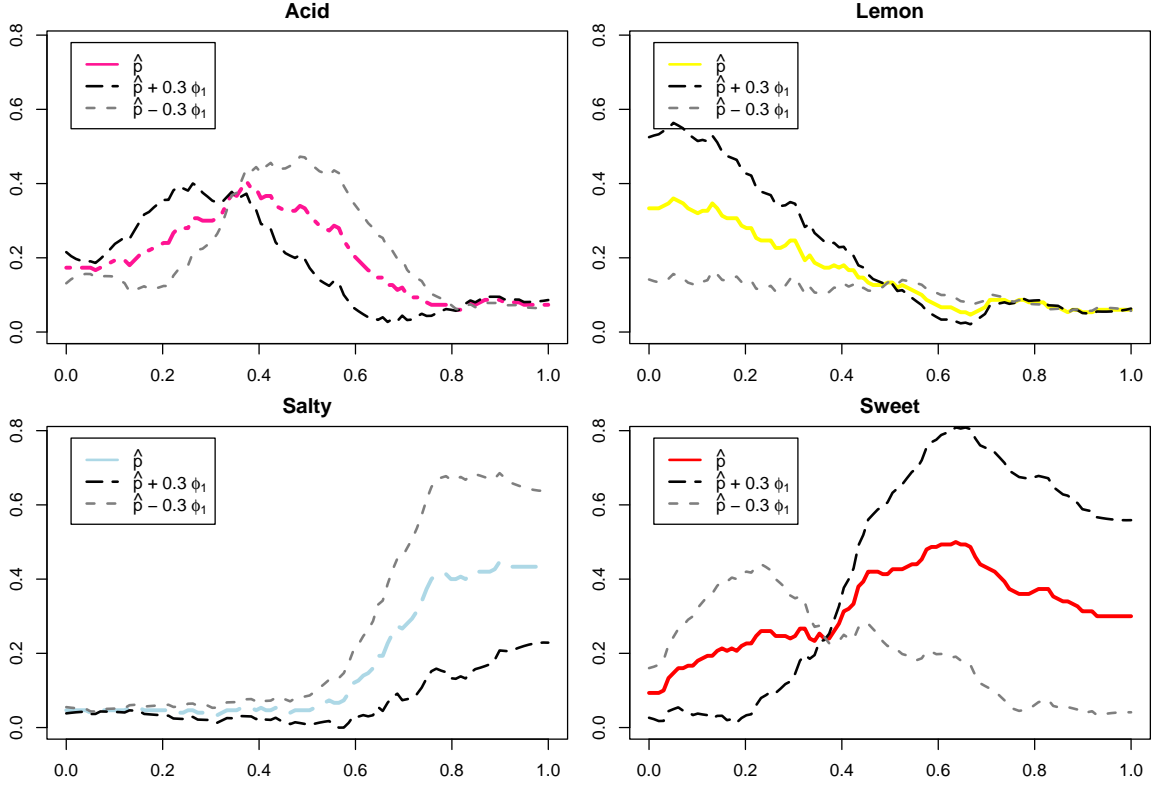


Figure 6: MFPCA with equal weights. First component. Variations around the probability of occurrence related to the first component of the Karhunen-Loève expansion, for the most important categories.

fifty panelists.

The mean trajectories  $\hat{p}_j(t)$  for each state  $j$  are presented in Figure 8. We can remark that their value is equal to 0 in the time interval  $[0, 0.2]$ . This corresponds to a latency time between the start of the tasting and the first click, corresponding to the occurrence of the first sensation. This latency time is removed in TDS to always have one descriptor selected, but it can be kept here. At the end of the tasting, all the descriptors are automatically unselected, which results in a zero mean value at time  $t = 1$ . The most frequently observed states are Lemon at the beginning of the period, followed by Acid, Sweet, and Salty at the end of the period, as in the TDS evaluations of the signals. As the result of the TCATA experiment can be considered as a set of  $q$  binary trajectories, MFPCA can be conducted on them. We have drawn in Figure 12 in the Appendix, the average number of selected states  $\sum_{j=1}^q \hat{p}_j(t)$  at each instant  $t \in [0, 1]$ . Contrary to TDS experiments in which the number of selected states is always equal to one, we note here a variation over time with a maximum value of 1.5 around time  $t = 0.6$ .

The first eigenvalue represents 19% of the total variance, whereas the second one represents 12 % of the total variance (see Figure 13 in the Appendix). As seen in Table 4 in the Appendix,

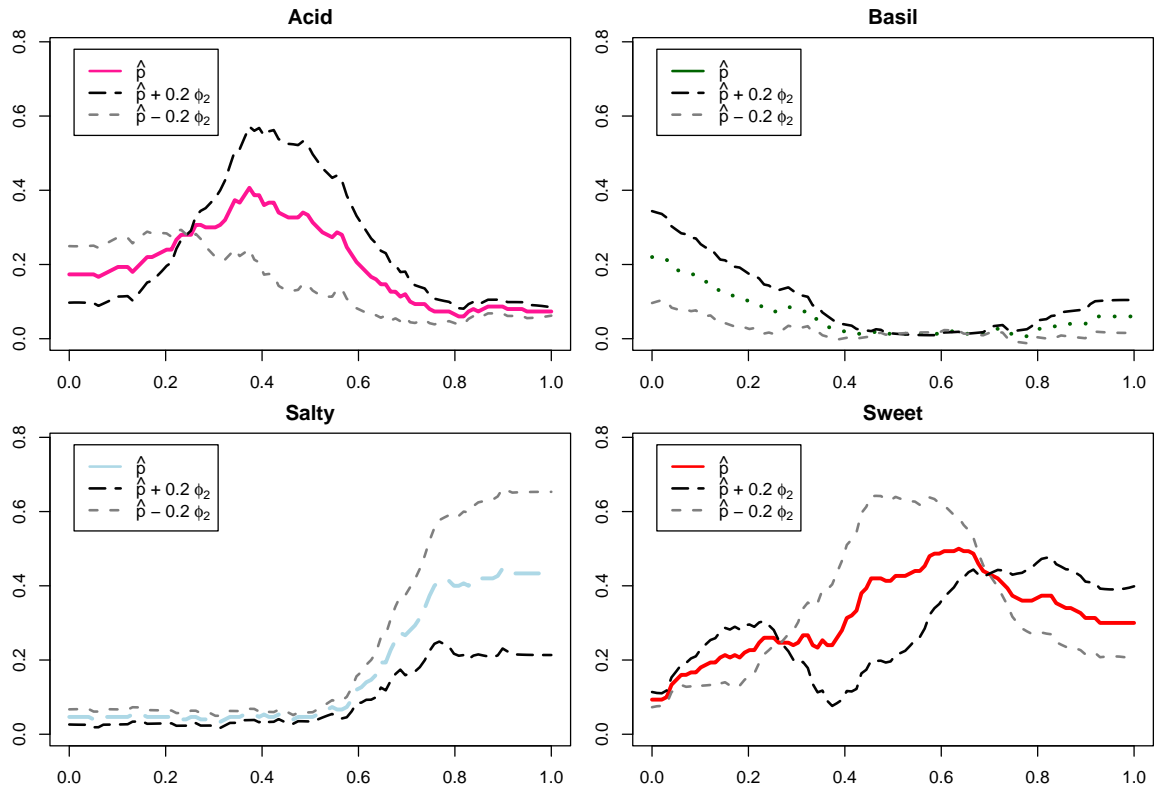


Figure 7: MFPCA with equal weights. Second component. Variations around the probability of occurrence related to the second component of the Karhunen-Loëve expansion, for the most important categories.

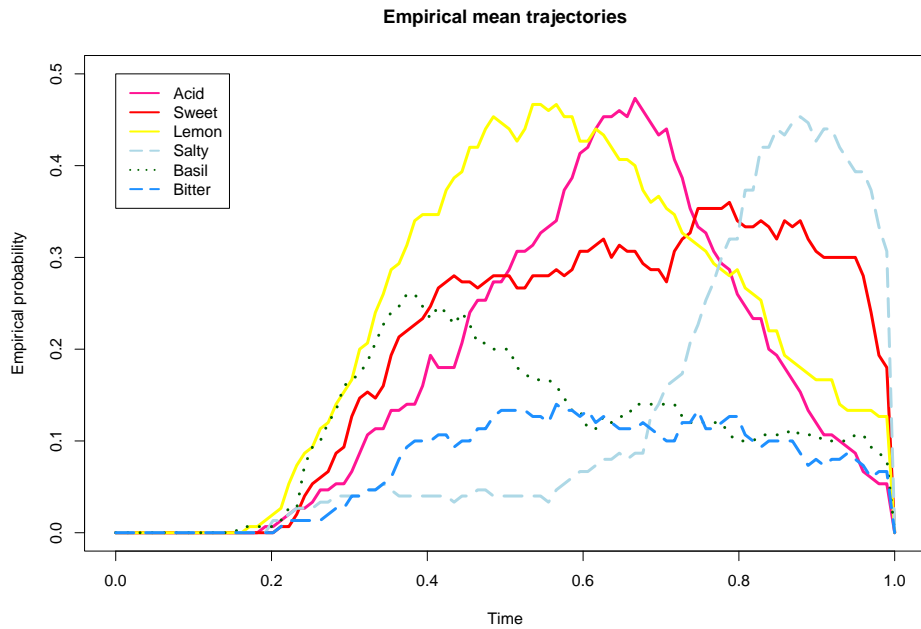


Figure 8: Empirical probability  $\hat{p}_j(t)$ ,  $t \in [0, 1]$  in TCATA experiments.

the importance of the different states is a slightly different compared to the analysis of TDS data in Section 4.1. We note that the Basil state appears to be important in both the first and second dimension, allowing to distinguish the S06 experiment, which is the only experiment with basil flavours, from the two other tasting experiments.

The estimated principal component scores are drawn in Figure 14 in the Appendix, whereas the main variations around the mean functions, for the first two dimensions, are drawn in Figure 15 and Figure 16 for the descriptors selected in TDS. The points corresponding to the S04 experiment are characterized by a first principal component score with positive values, related, as seen in Figure 15 to a high probability of occurrence of Lemon in the middle of the tasting, a small probability of occurrence of Acid at the end of the period, and a high probability of occurrence of Sweet and a small probability of occurrence of Salty at the end of the period. Nothing appears on the first component for Acid perception. On the second component, the same points have negative scores, showing a high probability of occurrence of Acid when  $t$  is larger than 0.5. The conclusions on the first two axes allow us to recognize the main structure of the original signal (see Figure 2). The same reasoning can be applied to S06 and S07, which are well discriminated by the first two dimensions of the principal components scores.

## 5 Concluding remark

The way, presented in this work, of reducing the dimension in a vector space of a panel of categorical trajectories allows for simple interpretation and comparison of individual trajectories. It is also direct to apply that methodology to other experimental protocols such as Temporal Check-All-That-Apply, in which  $X_j(t)$  and  $X_\ell(t)$ ,  $\ell \neq j$ , can be both equal to one at the same time  $t$ , whereas this would require to increase considerably the number  $q$  of states with continuous time correspondence analysis and Markov processes approaches. It can be easily extended to multivariate categorical trajectories and one could consider simultaneously, in our example, the three experiments made on the same panelists, that is to say  $\mathbf{Y} = (Y_{S04}, Y_{S06}, Y_{S07})$ . Finally, this dimension reduction approach can be useful to build predictive models, such as scalar-on-categorical functional data regression models, permitting to use categorical trajectories as explanatory variables in statistical models via the principal components scores. In the example presented in Section 4, it is not difficult to predict, with high accuracy, what is the underlying tasting experiment, among S04, S06 and S07, with a simple linear or quadratic discriminant analysis based on the principal components scores. This decomposition can also be useful to detect outlying trajectories.

**Acknowledgement** The Institut de Mathématiques de Bourgogne (UMR UB-CNRS 5584) receives support from the EIPHI Graduate School (contract ANR-17-EURE-0002).

## References

Aitchison, J. (1983). Principal component analysis of compositional data. *Biometrika*, 70:57–65.

Béno, N., Nicolle, L., and Visalli, M. (2023). A dataset of consumer perceptions of gustometer-controlled stimuli measured with three temporal sensory evaluation methods. *Data in Brief*, 48:109271.

Cardot, H. and Frascola, C. (2024). Hypothesis testing for panels of semi-markov processes with parametric sojourn time distributions. *J. Stat. Plann. Inference*, 228:59–79.

Cardot, H., Frascola, C., Schlich, P., and Visalli, M. (2019). Estimating finite mixtures of semi-markov chains: An application to the segmentation of temporal sensory data. *J. R. Stat. Soc., Ser. C, Appl. Stat.*, 68:1281–1303.

Castura, J., Antunez, L., Gimenez, A., and Ares, G. (2016). Temporal check-all-that-apply (tcata): A novel dynamic method for characterizing products. *Food Quality and Preference*, 47A:79–90.

Chiou, J., Chen, Y., and Yang, Y. (2014). Multivariate functional principal component analysis: A normalization approach. *Statistica Sinica*, 24:1571–1596.

Dauxois, J., Pousse, A., and Romain, Y. (1982). Asymptotic theory for the principal component analysis of a vector random function: Some applications to statistical inference. *Journal of Multivariate Analysis*, 12:136–154.

Deville, J. (1982). Analyse des données chronologiques qualitatives. *Annales de l'INSEE*, 45:45–104.

Deville, J. and Saporta, G. (1980). Analyse harmonique qualitative. In *Data Analysis and Informatics, Proc. Int. Symp., Versailles*, pages 375–389.

Gertheiss, J., Rügamer, D., Liew, B., and Greven, S. (2024). Functional data analysis: An introduction and recent developments. *Biometrical Journal*, 66:e202300363.

Greenacre, M. (2021). Compositional data analysis. *Annu. Rev. Stat. Appl.*, 8:271–299.

Happ, C. (2022). Mfpca: Multivariate functional principal component analysis. R package version 1.3-10.

Happ, C. and Greven, S. (2018). Multivariate functional principal component analysis for data observed on different (dimensional) domains. *J. Am. Stat. Assoc.*, 113:649–659.

Hsing, T. and Eubank, R. (2015). *Theoretical Foundations of Functional Data Analysis, with an Introduction to Linear Operators*. Wiley Series in Probability and Statistics. John Wiley & Sons.

Koner, S. and Staicu, A. (2023). Second-generation functional data. *Annu. Rev. Stat. Appl.*, 10:547–572.

Limnios, N. and Oprisan, G. (2001). *Semi-Markov processes and reliability*. Stat. Ind. Technol. Birkhäuser, Basel.

Lindsey, J. (2012). *Statistical analysis of stochastic processes in time*, volume 14 of *Camb. Ser. Stat. Probab. Math.* Cambridge University Press, Cambridge.

Peltier, C., Visalli, M., Schlich, P., and Cardot, H. (2023). Analyzing temporal dominance of sensations data with categorical functional data analysis. *Food Quality and Preference*, 109.

Pineau, N., Schlich, P., Cordelle, S., Mathonnière, C., Issanchou, S., and Imbert, A. (2009). Temporal dominance of sensations: Construction of the tds curves and comparison with time-intensity. *Food Quality and Preference*, 20:450–455.

Preda, C., Grimonprez, Q., and Vandewalle, V. (2021). Categorical functional data analysis. the cfda r package. *Mathematics*, 9(23):3074.

R Core Team (2024). *R: A Language and Environment for Statistical Computing*. R Foundation for Statistical Computing, Vienna, Austria.

Ramsay, J. O. and Silverman, B. W. (2005). *Functional data analysis*. Springer Ser. Stat. New York, NY: Springer, 2nd ed. edition.

Serfling, R. (1980). *Approximation theorems of mathematical statistics*. Wiley Ser. Probab. Math. Stat. John Wiley & Sons, Hoboken, NJ.

# Statistical description and dimension reduction of categorical trajectories with multivariate functional principal components

## Appendix

Hervé CARDOT and Caroline PELTIER

### A Analysis of TDS data considering weighted MFPCA

We also consider weights, defined in (10) and equal to  $w_j = \left( \int_0^1 \hat{p}_j(t)(1 - \hat{p}_j(t))dt \right)^{-1}$ , that give more importance to the states whose average variance is small, that is to say that are often or very rarely observed (see  $w_{p(1-p)}$  in Table 2 for the numerical values). As noted in Remark 2, considering these weights lead to impose the covariance operators  $\Gamma_{jj}$  to have the same trace. As seen in Figure 4 on the right, the decrease to zero of the sequence of eigenvalues  $\lambda_r$  is slower compared to previous analysis with equal weights. We draw in Figure 9 the first two principal components.

	Acid	Basil	Bitter	Lemon	Licorice	Mint	Salty	Sweet
$w_e$	0.12	0.12	0.12	0.12	0.12	0.12	0.12	0.12
$w_{p(1-p)}$	0.02	0.06	0.05	0.02	0.21	0.60	0.03	0.01
$w_p$	0.02	0.05	0.05	0.02	0.21	0.62	0.02	0.01

Table 2: Normalized (and rounded at two first digits in the Table) weights used for defining the inner product in  $\mathbb{H}$ .  $w_e$  corresponds to equal weights,  $w_{p(1-p)}$  to the scheme given in (10) and  $w_p$  to weights proportional to the inverse of the average probability of occurrence,  $w_j = \left( \int_0^1 p_j(t)dt \right)^{-1}$ .

The examination of the most important states (see Table 3) in the first and second dimension does exhibit some little difference with the case of equal weights. First Basil appears to be influential in the first and in the second dimension, amplifying the probability of occurrence for negative value of the first component and positive value of the second component (see Figure 10 and Figure 11) even if the weight  $w_j$  associated to this state is smaller in that unequal weights configuration compared to equal weights MFPCA. This makes it possible to identify, among the S06 tasting experiments, those in which the taste of basil was perceived. Another difference is the presence of Mint in the important variable, particularly on the second and third dimension whereas it was not present at all in the equal weights analysis.

If we consider weights that take account of the average probability of occurrence,  $w_j = \left( \int_0^1 \hat{p}_j(t)dt \right)^{-1}$ , we remark in Table 2 that those (normalized) weights  $w_p$  are very similar to

	dim 1	dim 2	dim 3
Acid	0.08	0.05	0.04
Basil	0.21	0.20	0.09
Bitter	0.00	0.02	0.14
Lemon	0.15	0.04	0.06
Licorice	0.01	0.02	0.01
Mint	0.00	0.22	0.56
Salty	0.19	0.36	0.05
Sweet	0.36	0.08	0.05

Table 3: Importance of the different states on each dimension of the MFPCA with weights given by (10).

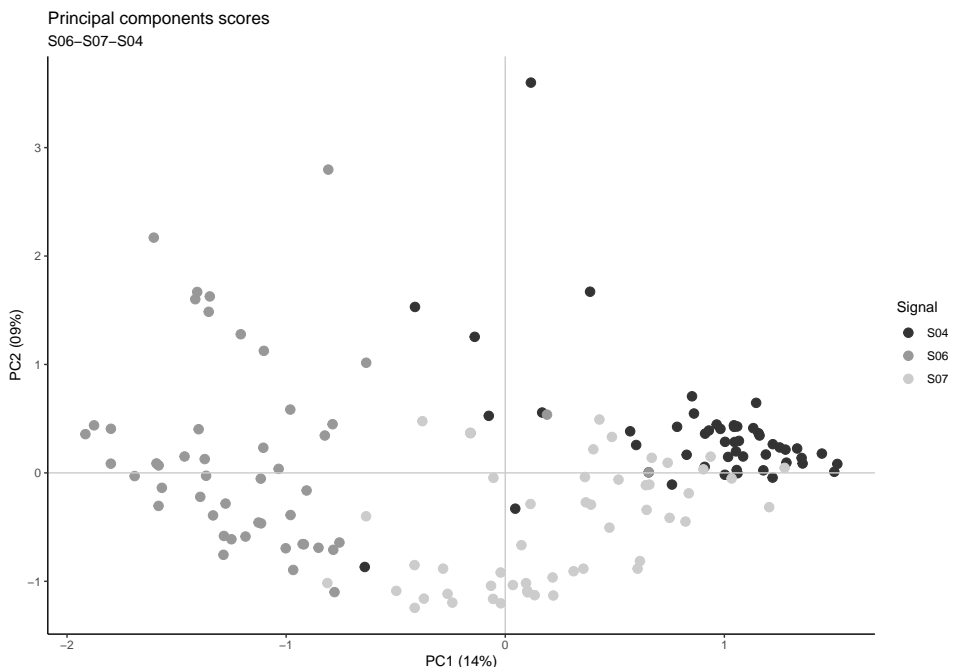


Figure 9: Estimated principal component scores with weights (10). Different colours are used to distinguish the observations according to the set of customer-controlled stimuli.

$w_{p(1-p)}$ , those given by (10). The decomposition of the trajectories are nearly the same and consequently not presented here.

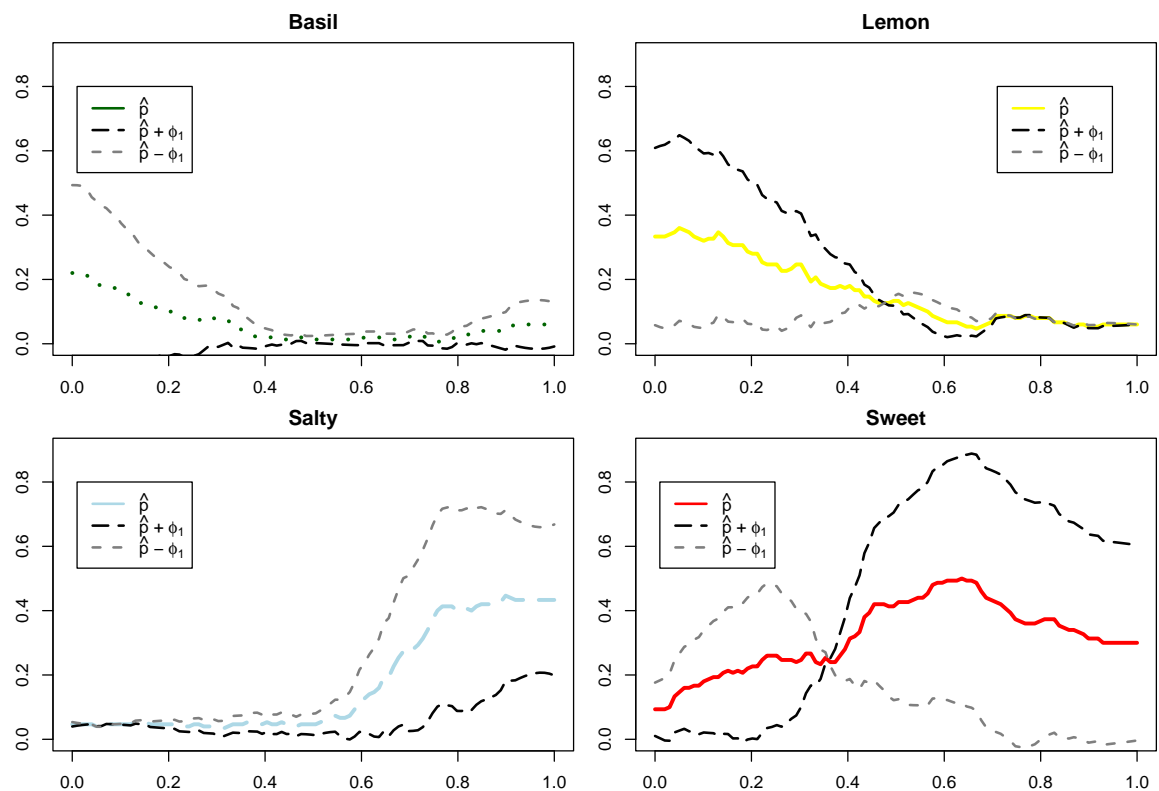


Figure 10: MFPCA with unequal weights (10). First component. Variations around the probability of occurrence related to the first component of the Karhunen-Loève expansion, for the most important categories.

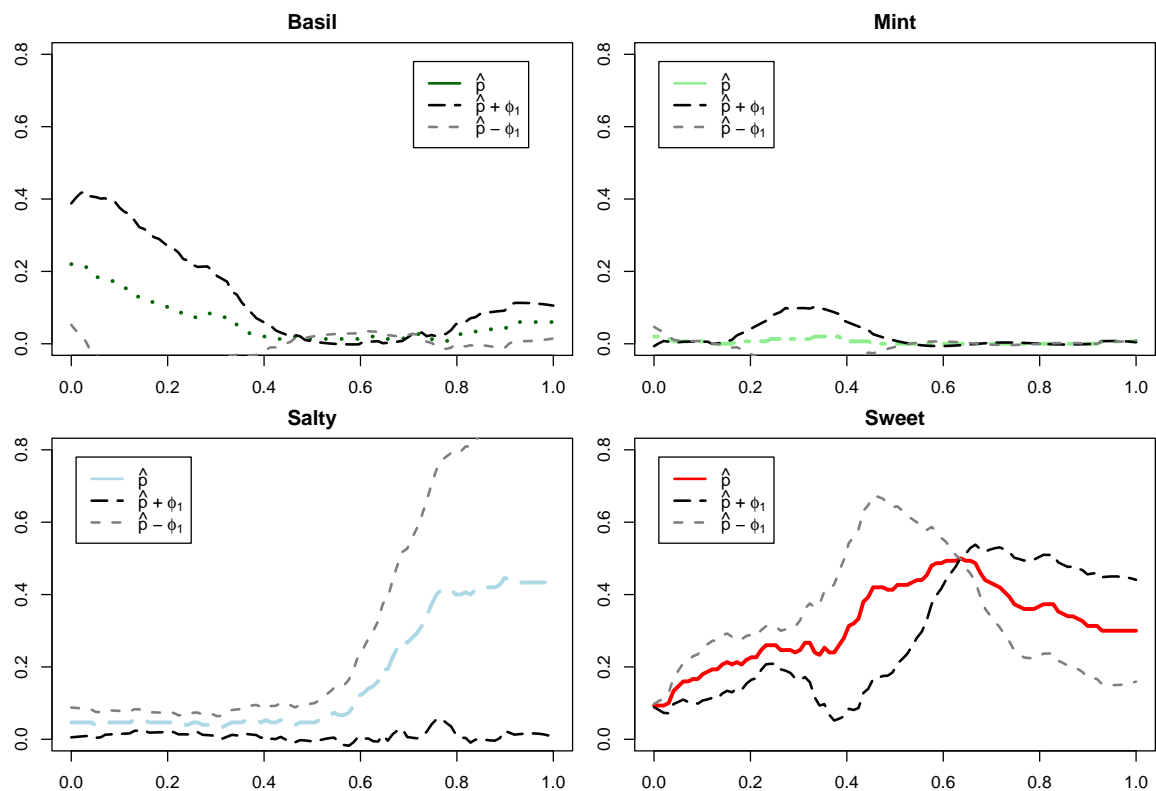


Figure 11: MFPCA with unequal weights (10). Second component. Variations around the probability of occurrence related to the second component of the Karhunen-Loëve expansion, for the most important categories.

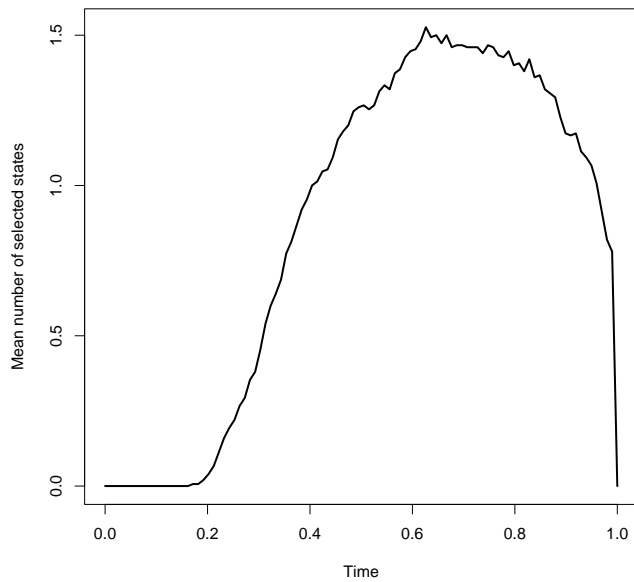


Figure 12: TCATA experiment. Representation of the mean number  $\sum_{j=1}^D \hat{p}_j(t)$  of selected states over time.

## B Additional tables and figures : TCATA experiments

	dim 1	dim 2	dim 3
Acid	0.00	0.35	0.20
Basil	0.19	0.19	0.04
Bitter	0.01	0.00	0.01
Lemon	0.27	0.11	0.39
Licorice	0.00	0.01	0.00
Mint	0.00	0.03	0.02
Salty	0.16	0.11	0.20
Sweet	0.36	0.19	0.14

Table 4: Importance of the different states on each dimension of the MFPCA of TCATA experiments, with equal weights.

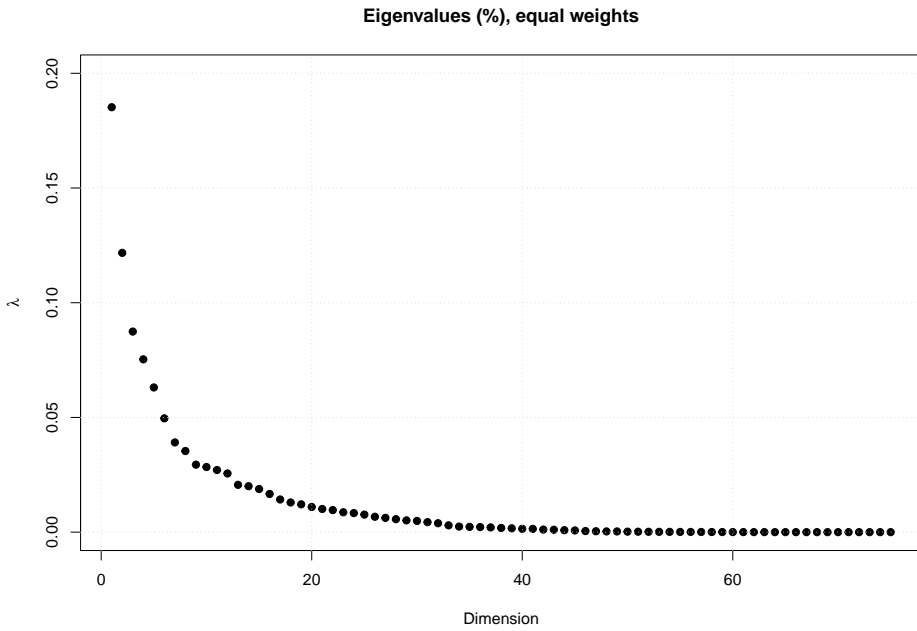


Figure 13: Proportion of total variance captured by the principal components considering equal weights for TCATA experiment.

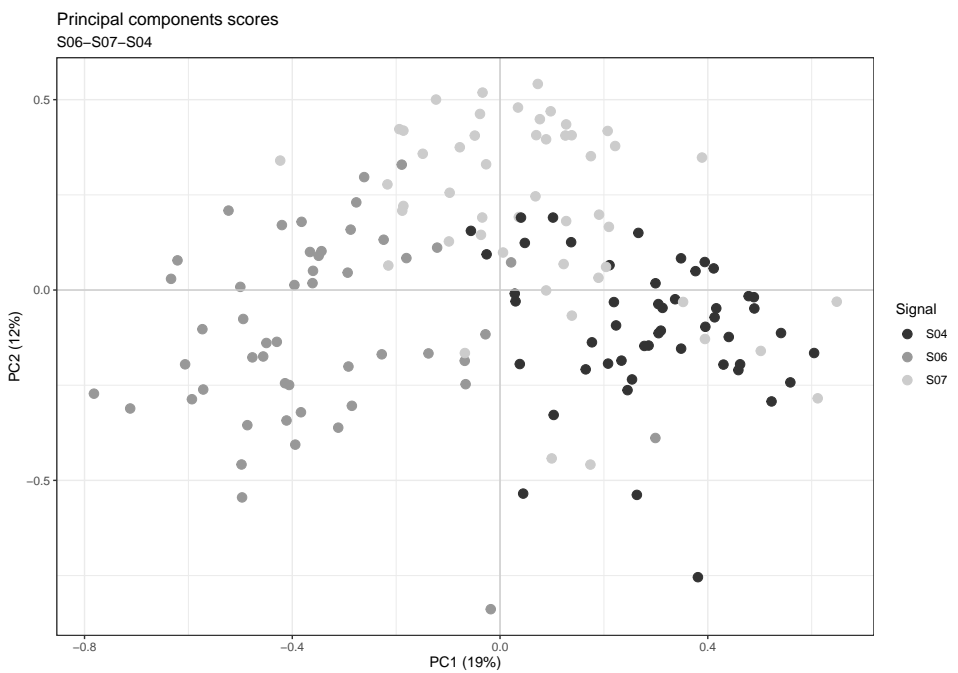


Figure 14: Estimated MFCPA scores with TCATA data. Different colours are used to distinguish the observations according to the set of gustometer-controlled stimuli

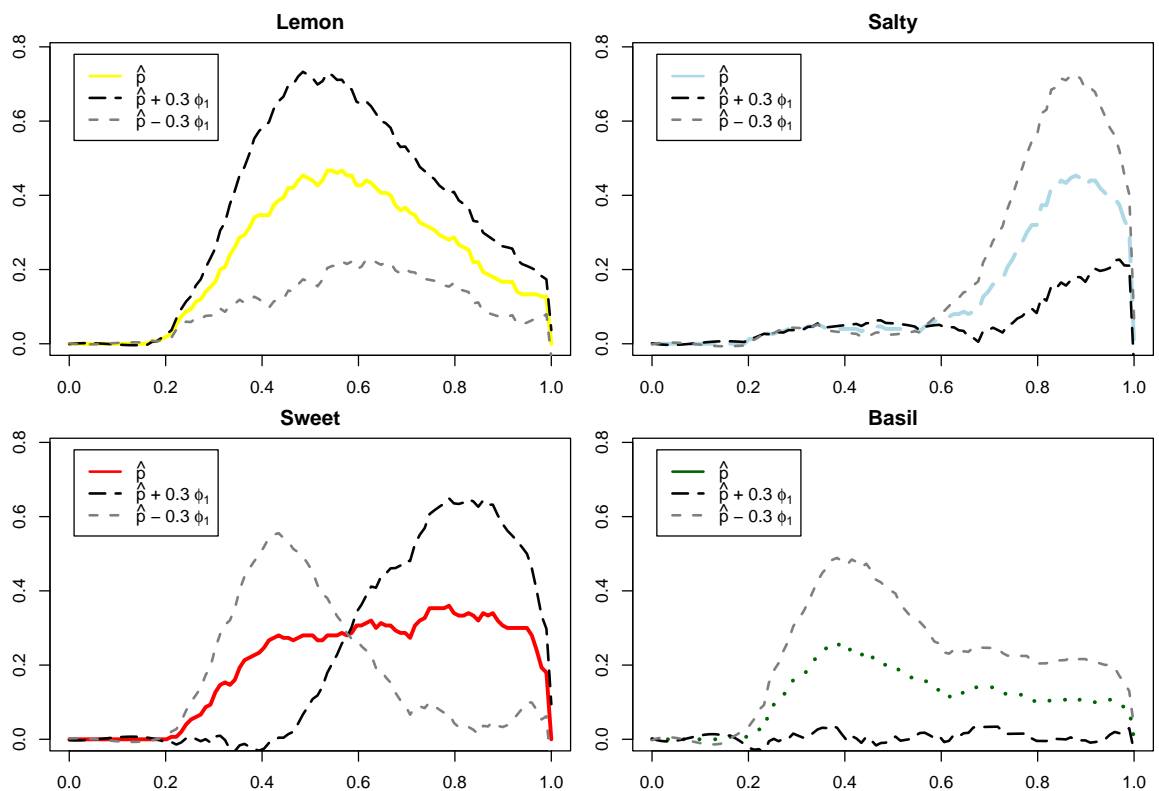


Figure 15: MFPCA of TCATA data. First component. Variations around the probability of occurrence related to the first component of the Karhunen-Loève expansion, for the most important categories.

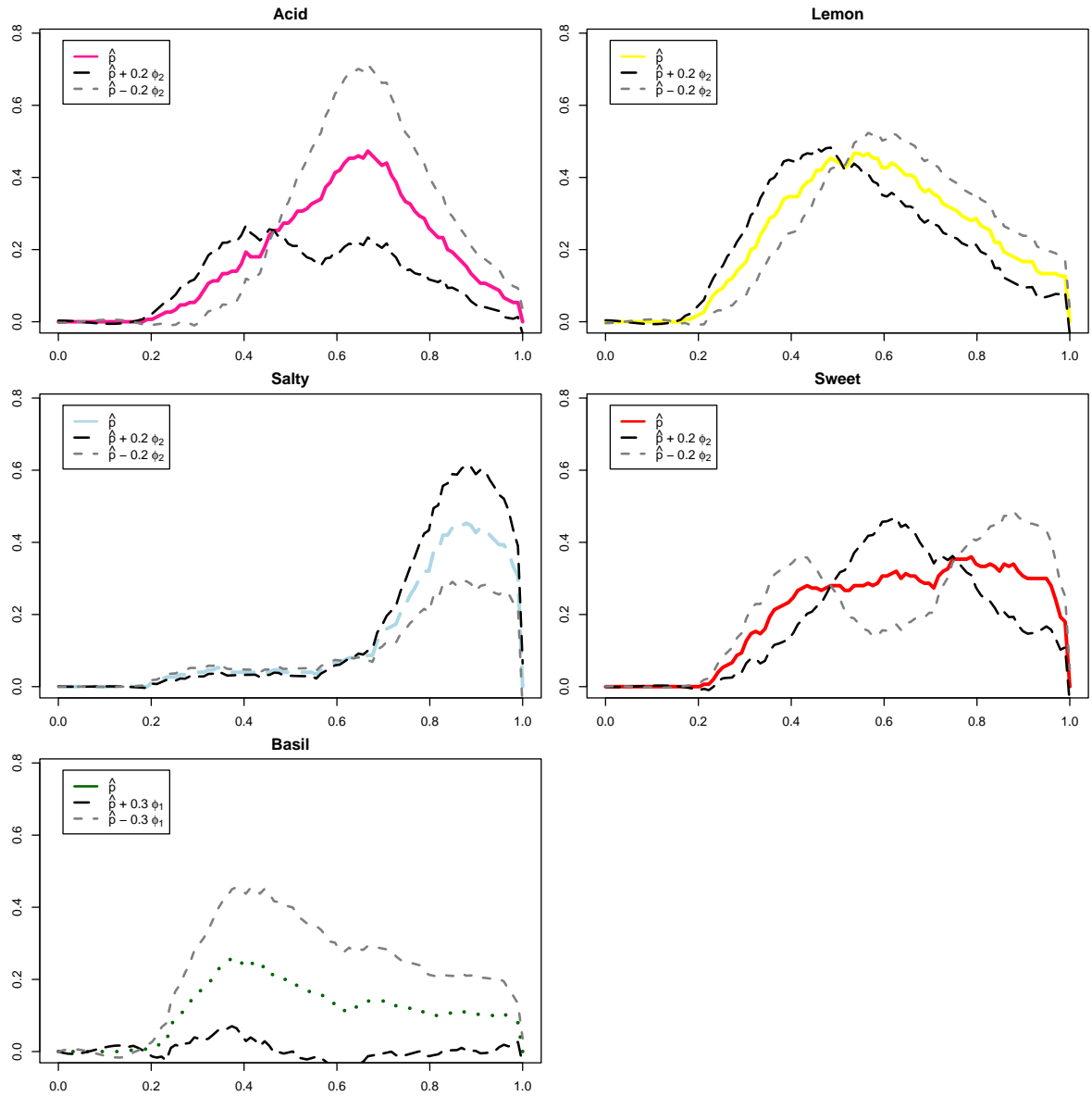


Figure 16: MFPCA of TCATA data. Second component. Variations around the probability of occurrence related to the second component of the Karhunen-Loeve expansion, for the most important categories